

Quantitative Colorimetric analysis of dye mixtures using an optical photometer Based on LED array

King-Tong Lau¹, William S. Yerazunis², Roderick L Shepherd¹, and Dermot Diamond^{1*}

¹National Centre for Sensor Research, Dublin City University, Republic of Ireland.

²Mitsubishi Electric Research Laboratory, Cambridge, Boston, USA.

Correspondence author: kim.lau@dcu.ie
dermot.diamond@dcu.ie

Summary

A disco photometer which was an optical sensing array based on multiple LEDs was constructed for colorimetric analysis. This approach has been used to analyse single dyes and dye mixtures containing up to three dye components. This technique made use of the inherent well-defined LED emission band to provide selectivity for chromophors, which have equally well-defined absorbance band to give very good analytical data. The results showed that this LED array configuration could be used to reduce the complexity of data obtained from the mixtures and also improve the quality of the output.

Keywords: colorimetric analysis, optical sensing, LED detector, multivariate analysis.

Introduction

In the area of chemical sensing it has always been a big challenge to analyse complex mixtures containing multiple components, which gives cross-sensitivities that interfere with the sensor performance. An ideal solution to this problem is to find sensors with very high selectivity, e.g. enzyme like specificity, to provide good analytical information from samples containing complex mixtures. Unfortunately, in general, a chemical sensor or even a reagent based sensing scheme can only achieve partial selectivity. To circumvent this problem, multiple sensors have been used to form sensor arrays that would provide a multi-dimensional information to describe the chemical signature of analytes. This information would be included into a reference library for the quantitative/qualitative determination of unknown samples. This multivariate approach is generally combined with a certain statistical method, normally a data reduction technique based on either linear or non-linear algorithms, such as principal component analysis [1] and neural networks [2,3], to simplify and improve the quality of the output. These approaches have been used successfully in chemical analysis and research efforts have continuously been made to improve the accuracy and reliability of the output. [4-6]

Chemical analysis using array sensing approach mainly includes electrochemical [7-9], mass [10,10] and optical sensors [12-18]. In the electrochemical sensing category a large proportion of the work has been in the area of gas sensing that is based on conductometric techniques. Sensors fabricated from inherently conducting polymers such

as polypyrrole and polyaniline [19]; polymer composites prepared from blending a conducting element such as carbon powder with a non-conducting polymeric binder [20] and semiconductors such as Tin oxide [21-24] have been extensively studied. Mass sensors are generally based on quartz crystals fabricated in a specific way so that they oscillate under applied voltage. The crystal is then coated with a sorbent material. The mass increase due to analyte being absorbed on the coating causes a frequency shift in the oscillator. Optical sensing using multivariate approach includes the use of fibre optics, [3-5] and chemochromic dyes [13,15]. Recent approaches include combining different sensors such as optical and capacitive in an array in an attempt to improve the reliability of the data [25,26]. These techniques normally provide qualitative rather than quantitative information, usually resulted in classification of chemicals.

Recently we have developed a simple optical sensor platform that used LEDs as both the light source and light detector. To function as a light sensor the LED is reverse biased at a specific voltage to generate photocurrent upon incident light. This photocurrent then discharges the LED at a rate that is proportional to the intensity of light reaching the detector. A simple threshold detection/timer circuit is used to indirectly measure the photocurrent at the detector LED to give digital output. [27] This LED emitter-light sensor combination is very versatile and can be configured to measure absorbance or reflectance and has been successfully used for colour measurements, and for monitoring colorimetric reactions and for metal detection. [28, 29]

This paper present the work on chemical sensing using a Disco photometer fabricated from LEDs. A series of LEDs with different emission bands were used as light sources, and a low band gap IR LED was used as a universal light detector. LED array was used as light source because they offer flexibility in emission wavelength from UV to IR range with variable spectral widths (emission band widths). An important criterion in constructing a sensing array is to achieve optimal selectivity. In this design we envisage to use the well-defined emission band of the light source, in this case the LEDs, to provide selectivity for the sensor array that measures absorbance or reflectance. The degree of overlapping between the absorption bands of the analytes and the emission band of the light source therefore determines selectivity of the sensing array. This simple concept makes use of the fact that the two parameters are both constant and well defined therefore the discrimination power of the array for target analytes can be tuned by selecting appropriate LED light sources to enhance selectivity. This approach does not rely on chemical selectivity of reagents such as chromophore receptors or fluorescent probes, which may become unstable overtime. An array of LEDs that covered a broad spectral range from UV to IR region was selected to demonstrate this flexible multivariate approach for quantitative analysis.

Experimental

Disco photometer

Super bright Infrared, Red, orange, yellow, green, blue and UV LEDs were purchased from Kingbright, USA. The characteristics of the LEDs are shown in Table 1 and Figure 2. The electronic circuitry used in this disco photometer has been described elsewhere [27]. The LEDs were arranged such that the emitter LEDs were encircling a centre detector LED protected by a black heat shrink to exclude the light coming in from the side as shown in Figure 1a. The emitter LEDs were inclined towards the centre so that all light beams merged at a spot approximately 1cm in diameter and 2cm from edge of the detector LED (Figure 1b).

Optical Cell

An optical cell was made up from a commercial black film canister ($d=3\text{cm}$, $h=5\text{cm}$) as shown in Figure 1b. A hole was cut on the top cover of the canister onto which the Disco photometer was secured using epoxy glue. To promote light reflection a white polypropylene sheet cut to size to fit the bottom of the canister was fixed in with epoxy glue. The distance from the tip of the LEDs to the bottom of the optical cell was 2cm where optimum reflection was obtained.

Dye solution Measurement

Methyl Red (MR), Bromocresol purple (BCP) and Aniline Blue (AB) were obtained from Aldrich, Dublin.

Three dye stock solutions, 0.05mM BCP, 0.05mM MR and 0.01mM AB were made up in 0.1M HCl. Mixing the dye stock solutions in various proportions made up multiple component samples that contained a mixture of dyes.

A fixed amount of 5ml solution was used for all measurements. For single component measurements, various dilutions were made up by mixing a predefined amount of the stock solution with 0.1M HCl to make up a final total volume of 5ml. For multiple component analysis, various ratios of stock solutions were used to make up a final volume of 5ml. One exception was that of the 1:1:1 mixture of the three dyes which was made up by mixing 1ml of each stock solution and made up to 5ml with 0.1M HCl.

A 5 ml sample of each solution to be investigated were pipetted into the optical cell and the top cover that was fitted with the disco photometer was then replaced. Three repeats of each sample were measured with data collection time set to 60s. The 7 emitter LEDs were configured to light up alternatively at a fixed rate of 1 pulse per second, and with the pulse width set at 100ms. The emitted light traveled through the sample from the LED down to the bottom of the cell modified with the white polypropylene sheet and then reflected back into the detector LED situated at the centre of the Disco photometer. The discharge time recorded by the detector LED was then transferred via RS232 port to the PC via the Hyperterminal software. The data was captured and saved as text files to be further analysed using MS ExcelTM. The sampling rate of the Discophotometer was approximately 8 data point per second from which the microprocessor produced a 16point average as the final output.

Results and Discussion

Data processing and selectivity

The photometer was configured to measure reflectance from a surface whereby the emitted light from the LEDs passed through the solution under investigation before reflected back from a white surface on the bottom of the cell to the detector. This approach is similar to a method that used an LED light source and an LDR (light dependence resistor) as the light detector for the detection of a metal ion [30]. Here, this optical device measures the time the reflected light discharges the detector LED. Taking the white reflected surface with the blank solution as reference to give the theoretical ideal reflectance, the discharge time measured is related to reflectance R by:

$$R = \frac{t_0}{t} \quad \text{eq. 1}$$

Where t_0 is the discharge time measured for blank solution and t is the discharge measured for samples.

In order to simplify the data interpretation, the absorbance (inverse of the reflectance) of the light passing through sample was used. Hence the raw data were process according to equation 2 to obtain the percentage relative absorbance values.

$$\% \text{ Relative Absorbance} = \frac{100 \times (t_{\text{sample}} - t_{\text{blank}})}{t_{\text{blank}}} \quad \text{eq. 2}$$

Where t_{sample} and t_{blank} is the discharge time measured for the sample and for the blank solution respectively. Therefore the final data output was the percentage relative absorbance with reference to the blank. Since weaker light intensity results in greater discharge time, therefore the values $(t_{\text{sample}} - t_{\text{blank}})$ are ≥ 0 . In this context, the expression shows that higher dye concentration results in more light being absorbed and leads to greater discharge time. When $t_{\text{sample}} \gg t_{\text{blank}}$ it may result in values greater than 100%.

This Disco photometer used an IR sensor LED as a universal light detector which does not provide any selectivity. Therefore the selectivity of this optical device relied solely on the degree of overlapping between the emission band of the LED light sources and the absorption band of the analyte species (i.e. the dyes). A selection of three dyes, namely, Methyl Red (MR), Bromocresol Purple (BCP) and Aniline Blue (AB), with overlapping absorption area between MR and BCP and between MR and AB as shown in Figure 2 were used to characterise the photometer. The anticipated selectivity of the system under

study can thus be deduced from the emission spectra of the LEDs used in the photometer together with the absorption spectra of the dyes, which are also shown in Figure 2.

Single component samples

The initial investigation was to calibrate three sets of solutions each containing various concentrations of a specific dye. To simplify the analysis these dyes were made up in 0.1M HCl to ensure only the acid form existed. Figure 3, calibration plots a-c were obtained from plotting the relative absorbance of the dye solutions obtained with equation 2 against their corresponding concentrations. Unfortunately, the LED #6 (with emission λ_{\max} at 565nm), which was supposed to be more sensitive to MR, did not behave at all due to an error during fabrication the angle of reflection was off-centred therefore the data was not useful at all. However, this draw back did not affect the overall performance of this array as the dye still absorbed sufficiently from LED#7. Actually, excluding LED#6, the emission of which would be absorbed by all three dyes, greatly simplifies the analysis of mixtures as will be shown later.

It can be seen that for the sample set containing MR solutions, only the light emitted from the LED #7 (with emission λ_{\max} at 465nm) was sufficiently absorbed. Similarly, strong absorptions from LEDs #7 and #8 emissions (λ_{\max} at 400nm and 465nm) for BCP samples, and absorptions from LEDs #3, #4 and #5 (λ_{\max} at 660nm, 630nm and 590nm) for AB samples respectively were observed. It was also observed that the responses of LED#8 in Figure 3b and LED#4 in Figure 3c deviated from linearity at higher dye concentrations, which was probably due to saturation at higher dye concentrations

The linear calibration plots shown in Figure 3 also inferred that quantitative information could be obtained by using data from individual LEDs. For example, a linear range between ca. 0-50 μ M with $R^2 = 0.999$ and an LOD of 3.3 μ M calculated using 3x standard deviation of the baseline for MR dye based on LED#7 (Fig. 3a) were observed. Similarly, a linear range of ca. 0-30 μ M with a calculated LOD value of 0.70 μ M for BCP based on LED #8 (Fig.3b); and a linear range between 0- 10 μ M with an LOD of 0.10 μ M for AB based on LED #3 (Fig.3c) respectively were observed. The differences between the LOD values reflected the different molar absorptivity of the analytes, which is in the order of AB>BCP>MR. Very low RSD values, typically < 1% for n=3, were obtained for all analysis, which suggested the data obtained from this optical photometer was very reproducible.

Quantitative Analysis of mixtures

Using this LED array approach with an appropriate selection of LEDs it is possible to obtain quantitative data from samples containing mixture of dyes. An ideal scenario is that each component of the mixture only absorbs emission from one LED from the array, which would make qualitative and quantitative analyses a simple task. This is not always possible in practice due to the availability of LED with the desire emission band or the dyes under investigation might have closely overlapping absorption band. However, with less complex samples, i.e. mixtures of around 2-4 components with known quality, provided that their absorption band are reasonably well separated and that a selection

LEDs with appropriate emission bands are available, it is possible to deduce the dye(s)' presence and also to evaluate their concentrations.

As the data obtained from an emission LED may contain absorption data from complex dye components, therefore the observed absorbance for each LED emitter can be expressed as:

$$A_{observed}^{LED\ i} = A_{dye\ 1}^{LED\ i} + A_{dye\ 2}^{LED\ i} + \dots + A_{dye\ n}^{LED\ i} \quad \text{eq.3}$$

where $A_{observed}^{LED\ i}$ is the observed absorbance from a mixture of dyes (i.e. dye1....dye n) using a particular emitter $LED\ i$. The absorbance from the same dye mixture for a different emitter $LED\ j$ will be expressed in a similar fashion.

For a non-selective system, i.e. when all LEDs are absorbed by all dyes, Eq. 3 suggests that the concentration of individual dye component is mathematically solvable provided that the number of LEDs that provides the absorbance data for the dye mixture matches the number of dye component. For a mixture of three dyes the minimum number of three LED is required to generate three equations to solve the problem. This will involve relatively simple algorithms even for more complex mixtures considering the current computing capability.

With careful selection of LEDs to provide better selectivity it is possible to simplify the data analysis. For example, as presented in this work, LED #8 is absorbed by only BCP, therefore,

$$A_{observed}^{LED\ \#8} = A_{BCP}^{LED\ \#8} \quad \text{eq.4}$$

whereas LEDs #3-5 are all absorbed by AB, so

$$A_{observed}^{LED\ \#3} = A_{AB}^{LED\ \#3} \quad \text{eq.5}$$

(LED#3 is chosen because it gave best range and sensitivity. LED#4 and 5 may be used to as comparisons to confirm the data obtained from LED#3.)

However, MR dye only absorbs from LED#7, which is also absorbed by BCP:

$$A_{observed}^{LED\ \#7} = A_{MR}^{LED\ \#7} + A_{BCP}^{LED\ \#7} \quad \text{eq.6}$$

Therefore for a mixture containing these three dyes, the concentrations of BCP and AB may be simply read out from the calibration curves from LED#8 and #3 respectively. The MR component may be deduced according to the following calculations:

1. Based on eq.4, estimate the correct BCP concentration using the calibration plot obtained for LED#8 shown in Figure 3b.
2. This estimated BCP concentration may then be fitted into the calibration curve obtained for LED#7, which is also shown in Figure 3b, to obtain the corresponding BCP absorbance value.
3. Absorbance due to the MR dye from LED#7 may then be obtained using eq.6.
4. The result obtained from 3 can then be fitted into the calibration curve shown in Figure 3a to estimate the concentration of the MR component.

This method of analysis was found to be useful for determining mixtures of known quality. Due to the selectivity offered by individual LED component, it was expected that improved accuracy might be obtained for the dye components that could be deduced from the absorbance data from a single LED. With more than one such LEDs it was possible to cross check the results to improve quality of output. This method also reduced the complexity of calculations for relatively complicated mixtures.

Table 2 summarised the results obtained from analysing fourteen samples of mixture that contained 2 and 3 dye components in various proportions using the method described above. Generally, the data obtained for the mixtures indicated that the estimated values matched well with the expected dye concentrations. For BCP and AB components in the mixtures, their concentrations were simply read off from the calibration curves according to eq. 4 and eq. 5 to result in good accuracy. As shown in Table 2 the % errors observed were small and were, on average, around 6%. Low standard deviations, typically within 5% RSD for $n=3$, were observed. For the determination of the MR component in the mixtures, the accuracy obtained were considerably higher with values ranging from 2% to 44%, and typically $>10\%$. Since these values obtained for MR were from mathematical elucidation, error propagation during the calculation procedures probably contributed mainly to the magnified errors. The small standard deviation values observed may support this hypothesis.

Overall this simple LED array selected to demonstrate quantitative analysis of dye mixtures have been successful. This model has shown that it is possible to reduce the complexity of the data obtained from a mixture by choosing appropriate LEDs. Hence simplifying data analysis and improve the quality of output. As expected, the data obtained from more selective, more direct source have been proved to be more accurate than those obtained using mathematical means. This supported the used of LEDs that were 'selective' to specific dye components.

The flexibility of LED based optical sensing array has also been demonstrated in this work. In this example, only 5 out of the 7 LEDs 'responded' to the samples and therefore the data obtained from the remaining two 'inactive' LEDs were discarded to simplify the analysis and to improve the quality of the output. For situations where more or less LEDs are required it is very simple to include or exclude the data collected from the range of LEDs present in the array. Moreover, it is easy enough to replace any LEDs by those that are more suitable for a specific application.

For further improvement of the sensing array, using LEDs with narrower band gaps (when available) could enhance the selectivity of the array; while increasing the number of LEDs within the array could improve the range of the absorbing species the array could detect. However, a balance between selectivity and coverage range must be maintained for this sensing approach to be effective and simple to use. Therefore the physical size of the array and the amount of data collected by the array should be considered; otherwise the device would become clumsy to operate. With the current computing technology the data from an array of up to 30 elements can easily be computed using inexpensive processors. The availability of surface mount LEDs, which are very small in sizes (typically surface area $< 1\text{mm}^2$) and with emission covering from UV to IR region implies that very small device could be fabricated from relatively large amount of LEDs. Hence an extensive and powerful LED based optical sensing array constructed with very inexpensive components is highly probable.

We envisage this LED arrays sensing technique be incorporated into instruments that use spectrophotometric technique for sample analysis. These would include HPLC, FIA, lap-on-a chip device, and optical biochips. Since this photometer measures reflectance rather than absorbance it is reasonable to propose that this LED array sensing approach could be applied to detect colour on a planar surface or to monitor the colour change of planar solid-state chemochromic sensors. Actually, works have already been undertaken to explore quantitative and qualitative analysis of solid-state chemical sensors. Furthermore, the LED emitters and detector(s) may be configured into many different designs in an optical cell to measure absorbance or reflectance.

Acknowledgement

The Authors wish to thank Science Foundation Ireland SFI for grant support under the Adaptive Information Cluster Award (SFI 03/IN3/1361).

References

1. Lau, K.T.; Micklefield, J.; Slater, J. M. *Sensors and Actuators B*, **1998**,50, 69-79.
2. McAlernon, P.; Slater, J. M.; Lau, K.T. *The Analyst*, **1999**, 124, 851-857.
3. Lyons, W.B.; Fitzpatrick, C.; Flanagan, C.; Lewis, E. *Sens. & Actuator A-Phys.* **2004**, 115, 267-272.
4. King, D.; Lyons, W.B.; Flanagan, C.; Lewis, E. *J. Meas. Sci. Technol.* **2004**, 15, 1560-1567.
5. Lyons, W.B.; Flanagan, C.; Lewis, E.; Ewald, H.; Lochmann, S. *Sens. & Actuator A-Phys.* **2004**, 114, 7- 12.
6. Ferreira, M.; Riul, A.; Wohnrath, K.; Fonseca, F.J.; Oliveira, O.N. Mattoso, L.H.C. *Anal. Chem.*, **2003**, 75, 953-955.
7. Gong, J.W.; Chen, Q.F.; Fei, W.F.; Seal, S. *Sens. & Actuator B-Chem.* **2004**, 102, 117-125.
8. Dable, B.K.; Booksh, K.S.; Cavicchi, R.; Semancik, S.T.I. *Sens. & Actuator B-Chem.* **2004**, 101, 284-294.
9. Riul, A.; Malmegrim, R.R.; Fonseca, F.J.; Mattoso, L.H.C. *Biosens& Bioelectron*, **2003**, 18, p. 1365-1369.
10. Wang, C.; He, X.W.; Chen, L.X. *Talanta*, **2002**, 57, P.1181-1188.
11. Lau, K.T.; McAlernon, P.; and Slater, J.M. *The Analyst*, **2000**, 125, 65-70.
12. Bacsik, Z.; Mink, J.; Keresztury, G. *J. Appl. Spectrosc. Rev.* **2004**, 295-363.
13. Feresenbet, E.B.; Dalcanale, E.; Dulcey, C.; Shenoy, D.K. *Sens. Actuator B-Chem.* **2004**, 97, 211-220.
14. Epstein, J.R.; Walt, D.R. *Chem. Soc. Rev.* **2003**, 32, 203-214.
15. Li, D.; Mills, C.A.; Cooper, J.M. *Sens. & Actuator B-Chem*, **2003**, 92, 73-80.
16. Zhang, L; Small, GW, *Appl. Spectrosc.* **2002**, 56, 1082-1093.
17. Grotti M. *Ann Chim-Rome*, **2004**, 94 (1-2): 1-15.
18. O'Farrel, I. M.; Lewis, E.; Flanagan, C.; Lyons, W.B.; Jackman, N. N. *Sens.& Actuators A-Phys*, **2004**, 115 (2-3): 424-433.
19. Riul, S. A.; Mello, A.M.G.; Bone, S.V.; Taylor, S.; Mattoso, L.H.C. *Synth. Met.*, **2003**, 132,109-116.
20. Ryan, M.A.; Lewis, N.S. *Enantiomer*, **2001**, 6, 159-170.
21. Riul, A.; Malmegrim, H.C.; dos Santos, R.R.; Carvalho, D.S.; Fonseca, A.C.P.L.F.; Oliveira, F.J.; Mattoso, L.H.C. *Sens. & Actuator B-Chem.* **2004**, 98, 77-82.
22. Mitzner, .KD.; Sternhagen, J.; Galipeau, D.W. *Sens. Actuator B-Chem*, **2003**, 93, 92-99.
23. Wollenstein, J.; Plaza, J.A.; Cane, C.; Min, Y.; Bottner, H.; Tuller, H.L. *Sens. & Actuator B-Chem*, **2003**, 93, 350-355.
24. Maekawa, T.; Suzuki, K.; Takada, T.; Kobayashi, T.; Egashira, M. *Sens. & Actuator B-Chem*, **2001**, 80, 51-58.
25. Hagleitner, C.; Hierlemann, A.; Lange, D; Kummer, A.; Kerness, N.; Brand, O.; Baltes, H. *Nature*, **2001**, 414, 293- 296.
26. Marcialis, G.L.; Roli, F.F.; *Pattern Recogn. Lett*, **2004**, 25 (11), 1315-1322.

27. Lau, K.T.; Baldwin, S.; Shepherd, R.L.; Dietz, P.L; Yerazunis, W. S.; Diamond, D. *Talanta*, **2004**, 63/1, 167-173.
28. Baldwin, S.; Lau, K.T.; Yerazunis W.S.; Shepherd, R.; Diamond, D. *IEICE transactions*, **2004**, Vol. E87-C, No.12 p.2099.
29. Lau, K.T.; McHugh, E.; Baldwin S.; Diamond, D. submitted to *Sens & Acts B* for publication.
30. Matias, F.A. A, Vila, M. M. D. C. and Tubino, M., *Sens & Acts B*, 88, **2003**, 60-66.

List of Figures and Tables

Figure 1. A picture of the Disco photometer (a) and a sketch of the Disco photometer to illustrate the light detection pathway (b).

Figure 2. Emission spectra of the LED light sources used in the photometer and the UV-VIS absorption spectra of Bromocresol purple (BCP), Aniline Blue (AB) and Methyl Red (MR) obtained from the original dye stock solutions made up with 0.1M HCl.

Figure3. Calibration plots obtained for (a) Methyl red, (b) Bromocresol purple and (c) Aniline blue using the disco photometer. The data were processed according to eq. 2 to obtain the relative absorbance value.

Table 1. Emission characteristics of the LEDs used in the fabrication of the Disco photometer and the absorption characteristics of the dyes used.

Table 2. Results obtained from analysis of 14 mixtures that contained 2 and 3 dye components.

Table 1.

LED/ (no.)	Spectral Line Half-width/nm	Peak emission Wavelength/nm
IR Sensor (1)	-	940
IR (2)	50	880
Red (3)	20	660
Orange red (4)	20	630
Yellow (5)	35	590
Green (6)	30	565
Blue (7)	25	465
UV (8)	26	400
Dye	Spectral half width of absorption/nm	Peak absorption Wavelength/nm
Methyl red	150	520
Bromocresol purple	100	430
Aniline Blue	100	600

Figure 1

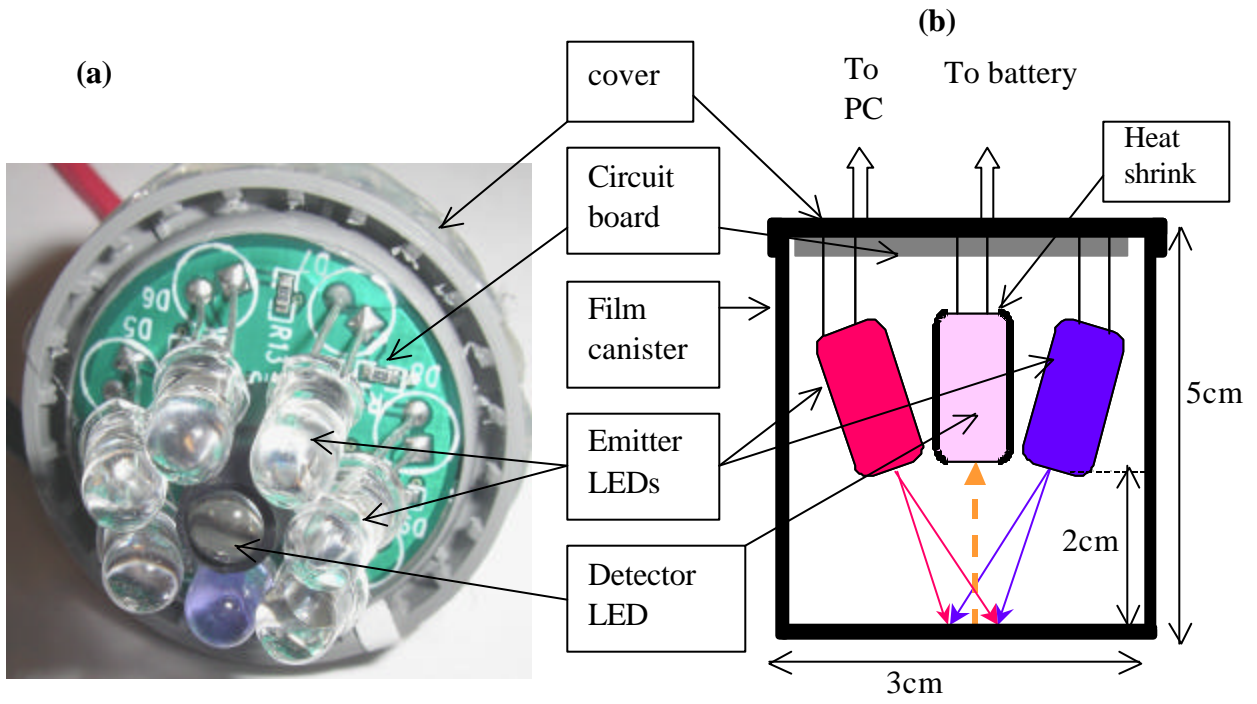


Figure 2

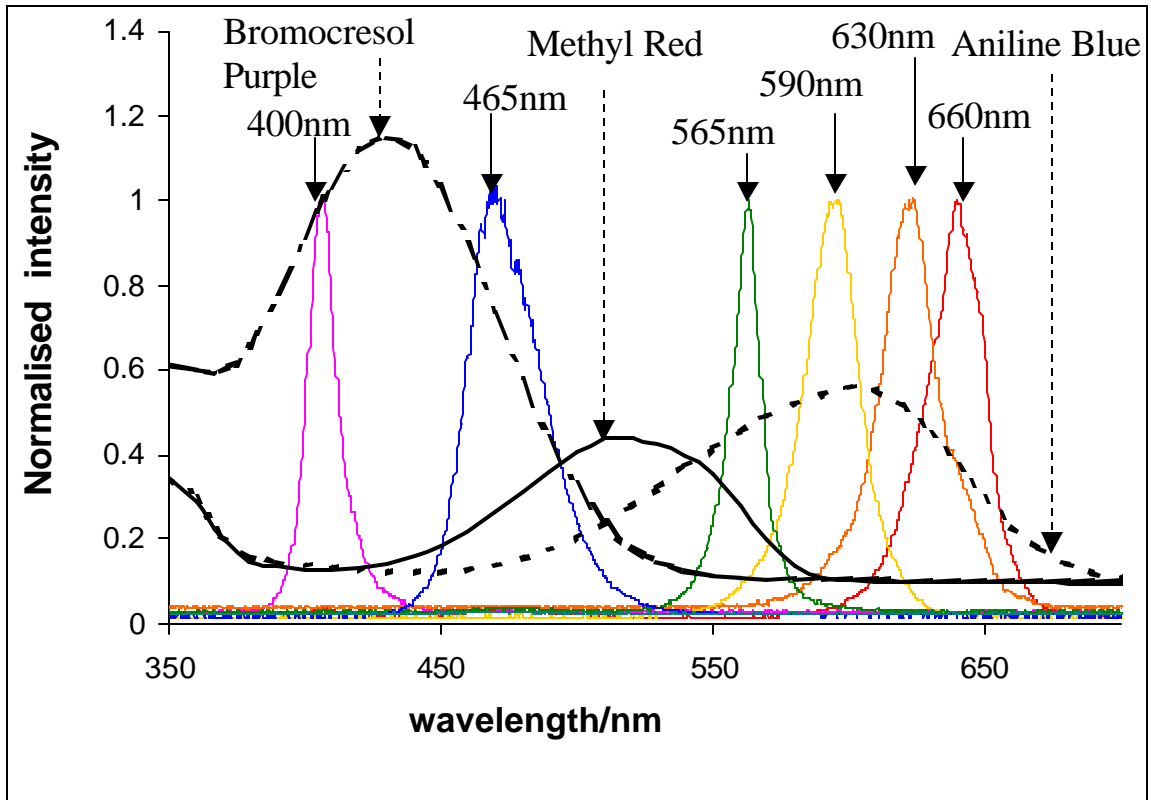


Figure. 3

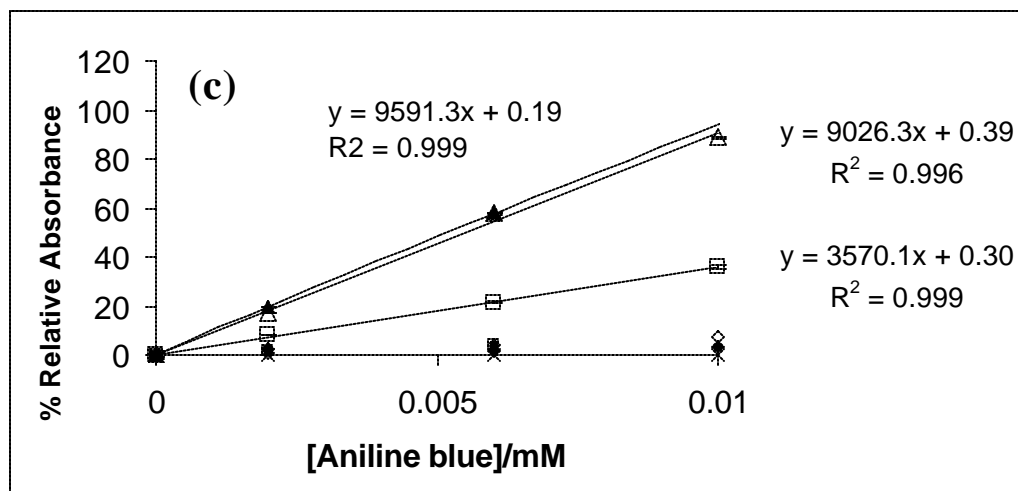
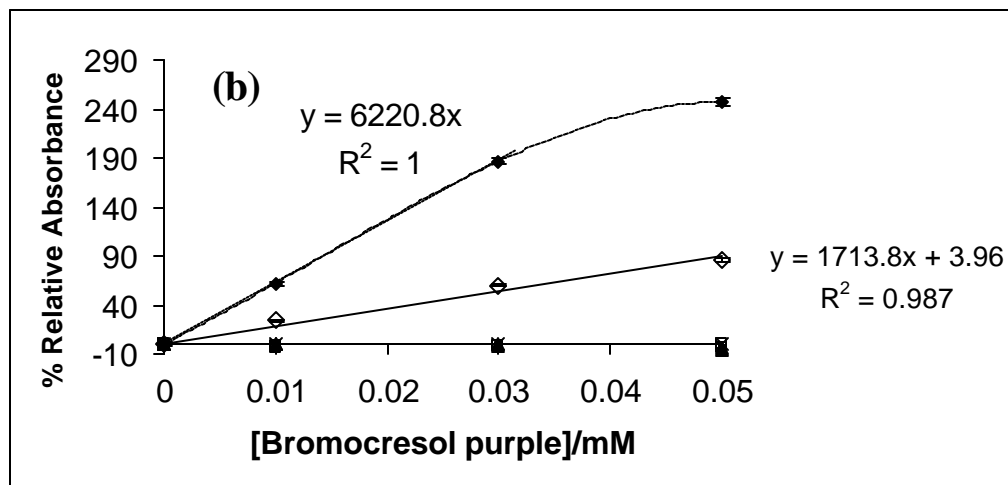
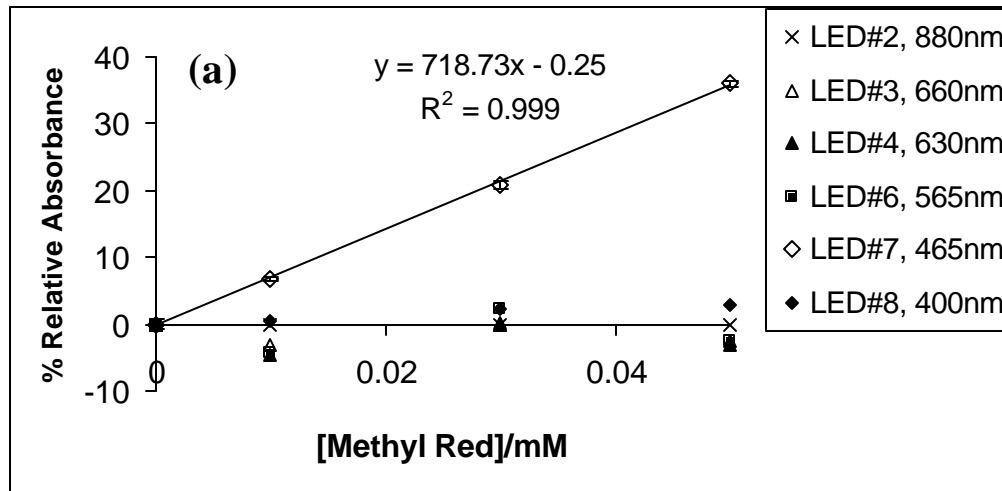


Table 2

Sample No.	Expected concentration/mM			Estimated concentrations/ mM (n=3)					
	MR	BCP	AB	MR	% Error	BCP	% Error	AB	% Error
1	-	40	2	-	-	37.32±0.52	6.7	1.9±0.04	4.2
2	-	20	60	-	-	20.73±0.28	-3.6	6.22±0.03	3.6
3	-	10	8	-	-	10.77±0.02	-7.8	8.35±0.01	-4.4
4	40	-	2	34.31±0.91	14.2	-	-	1.86±0.05	6.8
5	20	-	6	20.68±0.21	-3.4	-	-	6.13±0.0	-2.3
6	10	-	8	13.31±0.76	-33.1	-	-	8.37±0.02	-4.6
7	10	40	-	11.76±0.89	-18.0	35.3±0.31	11.6	-	-
8	20	30	-	17.50± 0.17	12.5	31.98 ±0.31	-6.6	-	-
9	40	10	-	34.24 ±1.29	14.3	11.31±0.43	-1.3	-	-
10	30	10	2	22.88 ±1.04	23.7	10.07 ±0.66	-0.7	1.70 ±0.03	14.9
11	10	30	2	5.58 ±0.43	44.2	31.87 ±1.34	-6.2	1.76 ±0.07	11.9
12	10	20	4	9.65 ±0.34	3.5	21.54 ±0.28	-7.7	3.87 ±0.12	3.3
13	10	10	6	9.79 ±0.64	2.1	10.76 ±0.46	-7.6	6.00 ±0.16	0.1
14	10	10	2	8.08 ±0.27	19.2	10.79 ±0.33	-7.9	1.73 ±0.05	13.3